PNAS
www.pnas.org

Supplementary Information for

Central human B cell tolerance manifests with a distinctive cell phenotype and is enforced via CXCR4 signaling in hu-mice

Thiago Alves da Costa, Jacob N Peterson, Julie Lang[1], Jeremy Shulman, Xiayuan Liang, Brian M. Freed, Susan A. Boackle, Pilar Lauzurica, Raul M. Torres, and Roberta Pelanda

Corresponding author: Roberta Pelanda (Roberta.Pelanda@cuanschutz.edu)

This PDF file includes:

Supporting Materials and Methods

Human subjects and samples

Human studies were approved by the University of Colorado Institutional Review Board and were performed in accordance with the Declaration of Helsinki. Pediatric bone marrow biopsy specimens were provided by the Pathology lab of the Children's Hospital of Colorado after examination was completed and these specimens were ready to be discarded. These specimens were received as de-identified samples (Table S1) 1-3 days after collection, and were stained and analyzed by flow cytometry immediately or at a later time point after freezing and thawing. None of the samples analyzed for this study displayed by flow cytometry unusual B cell clonal cell expansions indicative of tumor. Healthy cord blood samples (CBH) were donated by the University of Colorado Cord Blood Bank at ClinImmune Labs (Aurora, CO) as de-identified samples that were rejected by the bank due to low volume or other reasons. These samples were collected following receiving informed written consent and a strict screening process that recruited only subjects without personal and family history of immunological disorders and/or blood cancer. "Autoimmune" cord blood samples (CBA) were obtained after the consent of subjects (pregnant women) with a diagnosis of systemic lupus erythematosus, rheumatoid arthritis, or type-1 diabetes (described in Table S2). These subjects were recruited at the Colorado University Hospital (UCH) either among Rheumatology pregnant patients or directly in the labor ward. Gestation was between 35 and 39 weeks, and both vaginal and C-section births were included. Clinical status of subjects recruited in the labor ward was diagnosed at UCH or by other medical providers. The CB samples were stored at room temperature and processed within 2 days from collection. Diagnostic PCR of the PTPN22 alleles encoding the R620 or W620 variants was performed according to a published protocol (1) on genomic DNA extracted from the CB samples. CB mononuclear cells were isolated over a Ficoll-density gradient. $CD34^+$

hematopoietic stem cells were purified from the CB mononuclear cells using the human $CD34^+$ MicroBead Kit (Miltenyi Biotec), and were then expanded in culture for 5 days as previously described (2, 3). Cells were stored at –80ºC and thawed just before their injection into mice.

Development and treatment of HIS hu-mice

BALB/c-$Rag2^{null}$Il-$2r\gamma^{null}$$Sirpa^{NOD}$ (BRGS) mice (4, 5) and Hcκ7-Tg/+ (Hcκ+) BRGS mice (6) were bred to produce Hcκ+ and Hcκ– BRGS littermates. Genotyping was performed by PCR on genomic DNA isolated from a tail clip at time of weaning as previously described (6). The mice were maintained under Specific Pathogen Free (SPF) conditions in the Vivarium of the University of Colorado Denver Anschutz Medical Campus (UCD-AMC) in Aurora, CO on a diet that alternated every two weeks between regular chow and a Septra-enriched chow (Envigo). For the generation of HIS hu-mice, 1 to 3-day old Hcκ+ and Hcκ– BRGS pups were sub-lethally irradiated with 300 rad and injected within 4 hours with 100,000 to 400,000 $CD34^+$ cells isolated from either CBH or CBA human umbilical cord blood samples. The cells were injected i.v. in the facial vein or, less frequently, directly into the liver. Blood samples were collected at 10 weeks of age to assess human hematopoietic chimerism (%$hCD45^+$/%$hCD45^+$+$mCD45^+$) and recipients with less than 5% chimerism were removed from the study. HIS hu-mice were euthanized for tissue analyses at 13 to 15 weeks of age, a time representing an optimal window for the investigation of B cell development (3, 6). The anti-hCD69 2.8 monoclonal antibody (mAb) was generated, tested and kindly provided by Dr. Pilar Lauzurica (7). Hu-mice were given one i.p. injection of 500 μg of anti-hCD69 2.8 mAb in PBS (or PBS control) and analyzed 48 hours later. Some groups of hu-mice were injected i.p. with 100 μg of AMD3100 (Calbiochem) in PBS, or PBS alone, either once

and analyzed 48 hours later, or 5 times over the course of 24 hours and analyzed one hour after the last injection. These treated hu-mice were also bled 24 hours before and after starting the treatments to investigate κ^+ cell frequency and phenotype in the blood. At experimental endpoint, HIS hu-mice were euthanized, and their tissues were harvested for analysis. Animal procedures were approved by the University of Colorado AMC Institutional Animal Care and Use Committee.

Cell staining and Flow cytometry of hu-mice

Bone marrow, spleen, lymph node and blood tissues from HIS hu-mice were processed into single-cell suspensions and cells were counted with a hemocytometer under a microscope. Blood mononuclear cells were separated over a Ficoll-Plaque gradient. Cells were stained in staining buffer (PBS, 1% BSA, 0.1% NaN_3) with antibodies specific for hCD3 (HIT3a), hCD10 (H110a), hCD14 (M5E2), hCD19 (HIB19), hCD20 (2H7), hCD24 (ML5), hCD33 (P67.6), hCD45 (HI30), mCD45.2 (104), hCD69 (FN50), hCD81 (5A6), hCXCR4 (12G5), mCXCR4 (L276F12), hIgD (IA6-2), hIgκ (MHK-49), and hIgM (MHM-88), from BioLegend; hCD19 (SJ25C1), hCD38 (HB7), hIgλ (JDC-12), and hS1PR1 (SY4GYPP) from BD Biosciences; hBAFFR (FAB1162A) from R&D Systems, phospho-ERK1/2 (197G2), and secondary goat anti-rabbit IgG polyclonal antibody from Cell Signaling. For the intracellular detection of proteins (Igκ and Igλ), cells were first stained for surface molecules, then fixed in 2% formaldehyde and permeabilized with 0.5% Saponin (Sigma-Aldrich) before staining with antibodies resuspended in 0.5% Saponin. For detection of phospho-ERK (pERK), cells were first rested for 1h at 4ºC in HBSS with Ca^{+2} and Mg^{+2} (Cellgro) with 1% FBS. Cells were then treated with 60 μM sodium pervanadate for 5 min at 37ºC, fixed in 2% formaldehyde, permeabilized with 90% methanol and stained with anti-pERK or isotype control antibodies. For the

detection of human S1PR1, cells were incubated for 30 minutes and then stained with anti-hS1PR1 antibody (clone SY4GYPP) from BD Biosciences (8) in PBS buffer containing 1% fatty acid-free BSA to allow for recycling of intracellular S1PR1 to the cell surface (9). Live/dead cell staining was performed using Zombie Green Fixable Viability Kit (BioLegend) according to manufacturer's instructions. Cell data were collected on a BD LSRFortessa Flow Cytometer (BD Biosciences) and were analyzed with FlowJo v10.7.1 software (FlowJo, LLC/BD, formerly Tree Star Inc., Ashland, OR, USA).

Cell migration assay

The cell migration assay was setup based on previous reports (10-12). Bone marrow cells isolated from Hcκ+ HIS hu-mice were resuspended and incubated for 30 min at 37ºC in migration medium (IMDM supplemented with 1% fatty acid-free BSA, glutamine, penicillin and streptomycin). Cells were washed once with migration medium, resuspended at $1X10^6$ cells/100 μl in migration medium and plated in duplicate top wells of a 5 μm-pore Costar transwell 24 well plate (#CLS3421). The bottom wells were plated with 500 μl of migration medium containing or not 0.3 μg/ml of human CXCL12 (R&D). After 3 hours incubation at 37ºC, cells were removed from the upper and lower wells and stained in one step for surface markers only, to reduce cell manipulation and loss during the staining procedure. Cells were stained for hCD45, CD19, CD24, CD81, CD69, IgM, mCD45, CD3, CD14, CD33, and 7AAD, and then collected on a BD LSRFortessa for analysis and counting. After gating out $mCD45^+CD3^+CD14^+CD33^+7AAD^+$ cells, remaining cells were analyzed to gate $CD24^{high}$ cells that were $CD19^{high}IgM^+$ (nonautoreactive, NA, cells), $CD19^{low}IgM^-CD81^{low}CD69^+$ (autoreactive, AUT, cells), and $CD19^{high}IgM^-CD81^{high}$ (pro&pre-B cells). The number of events collected over 80 sec for each of these populations was used to calculate cell migration. The % migration for each

sample well was calculated as (number of cells in lower well)/(number of cells in lower+upper wells) x 100. Results from both wells for each cell sample were graphed because this assay suffers of high variability within an experiment and between experiments.

Treatment and analysis of mice

Immunoglobulin knock-in mice 3-83Igi,H-2^d (nonautoreactive strain) and 3-83Igi,H-2^b (autoreactive strain) mice (13, 14) and wild-type CB17,$H2^b$ mice were bred and maintained in a specific pathogen-free facility at the University of Colorado Anschutz Medical Campus Vivarium (Aurora, CO). All animal procedures were approved by the UCD Institutional Animal Care and Use Committee. Groups of 5-7 weeks old mice were injected i.p. with 120 μg of AMD3100 (Calbiochem) in PBS, or with PBS alone, either one time and mice analyzed one hour later, or 4 times over the course of 24 hours and mice analyzed one hour after the last injection. Blood, bone marrow, and spleen cells were isolated for analyses after euthanasia. Single-cell suspensions were stained with fluorochrome-conjugated antibodies against mouse B220 (RA3-6B2), IgD (11-26c-2a), IgM (MHM-88), Igλ (RML-42), CD2 (RM2-5), CD3 (145-2C11), CD19 (1D3), CD21 (7E9), CD23 (B3B4), CD24 (M1/69), CD34 (561), CD69 (H1.2F3), CD81 (Eat-2) purchased from eBioscience, BD Pharmingen, or Biolegend. The fluorescent chemical compound 7-Aminoactinomycin D (7AAD; eBioscience) was used to discriminate dead cells. Cell data were collected on a BD LSRFortessa Flow Cytometer (BD Biosciences) and were analyzed with FlowJo v10.7.1 software (FlowJo, LLC/BD, formerly Tree Star Inc., Ashland, OR, USA). Analyses were performed on live cells based on lack of 7AAD incorporation. Cell doublets were excluded based on FSC-A versus FSC-H scatter plot.

ELISAs

Total serum Igκ and Igλ of HIS hu-mice were measured by ELISA as previously described (6). Briefly, 96-well Nunc-Immuno MaxiSorp plates (Thermo Fisher Scientific) were coated overnight at 4°C with 10 μg/ml of mouse anti-human Igκ (SB81a) or Igλ (JDC-12) (Southern Biotechnologies Associates). The following day, plates were washed four times in PBS Tween 0.1% and blocked for 2h at room temperature with PBS 1% BSA, 0.1% NaN_3. Plates were then washed three times and hu-mouse sera added to the plates at threefold serial dilutions starting at 1:10 dilution. Standard hIgM or hIgG was added to plates starting at 5 μg/ml. Plates were then incubated overnight at 4°C and subsequently washed five times. Human Igs on plates were detected by incubating for 2h at 37ºC with alkaline phosphatase (AP)-conjugated mouse anti-human IgM (UHB) or IgG (H2) (Southern Biotechnologies Associates) diluted at 1:500. After washing four times, plates were developed by the addition of AP's substrate (Sigma-Aldrich) solubilized in 0.1 M diethanolamine and 0.02% NaN_3. Light absorbance was measured at OD_{405} multiple times with a VersaMax plate reader (Molecular Devices). Data were analyzed with the SoftMax Pro software v6.4.2.

Statistical analysis

Statistical significance evaluation was performed with GraphPad Prism software using two-tailed t-test when comparing two groups or Analysis of Variance (ANOVA) when comparing three or more groups/variables. When ANOVA was used, multiple comparisons between the groups was performed with the Uncorrected Fisher's Least Significance Difference (LSD) test. The level of significance was: *$p<0.05$; **$p<0.01$; ***$p<0.001$; ****$p<0.0001$. Data in graphs is represented as mean±SD.

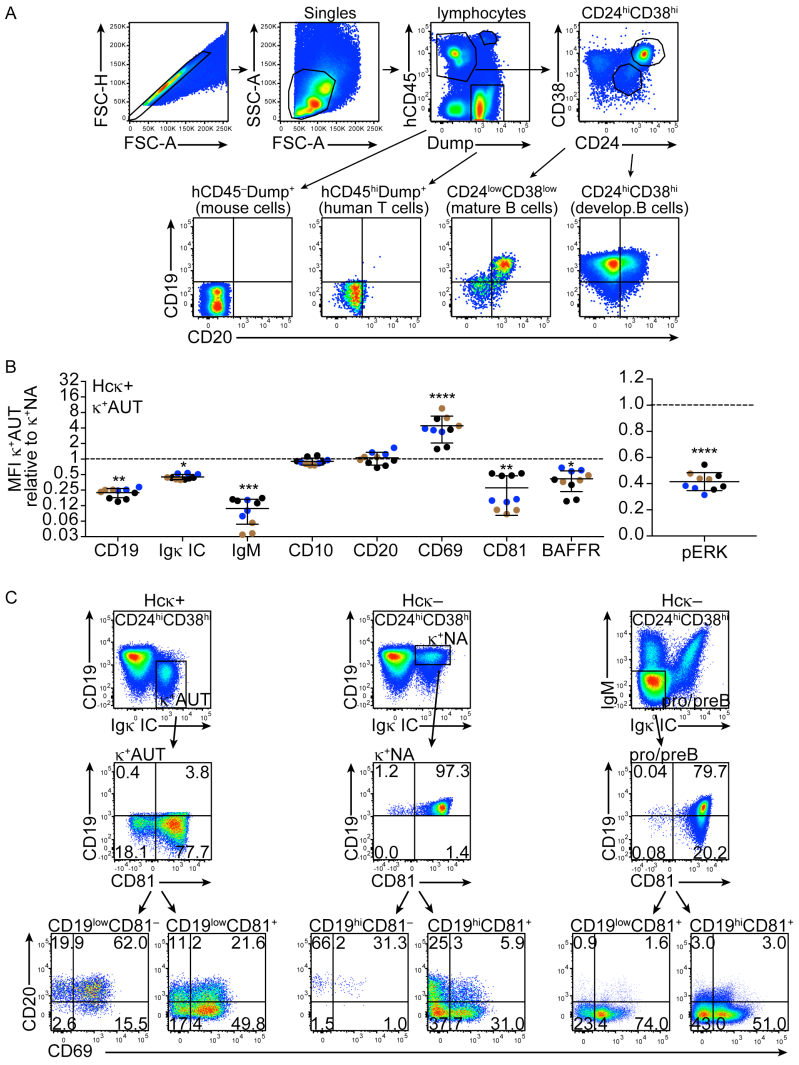

Fig. S1. Analyses of κ+ autoreactive and nonautoreactive human B cells from individual Hcκ+ and Hcκ– hu-mice.

A) Top plots: strategy for gating human CD24^{hi}CD38^{hi} developing B cells in the bone marrow of HIS hu-mice (13-15 weeks after the engraftment of hHSCs). Bottom plots: analysis of CD19 and CD20 expression by the CD24^{hi}CD38^{hi} cell subset in comparison to other cell populations gated as shown on top plots. “Dump” includes a dead cell dye and antibodies for hCD3 (human T cells), hCD14 and hCD33 (human monocytes and macrophages), and mCD45 (mouse hematopoietic cells) all in the same fluorescent channel. B) Relative geometric mean fluorescence (MFI) intensity values of indicated

molecules expressed by κ^+AUT immature ($CD24^{hi}CD38^{hi}$) B cells of individual Hcκ+ hu-mice. To obtain the relative MFI, the MFI value for each sample was divided by the average MFI of the κ^+NA samples from Hcκ– hu-mice that were analyzed on the same day. Each symbol represents a mouse and the different colors represent distinct cord blood units used to generate independent groups of HIS hu-mice. Horizontal and vertical lines in all graphs represent mean±SD. N=10 Hcκ+ and N=9 Hcκ– hu-mice from 3 groups, respectively. Statistical analysis was performed with two-way ANOVA multiple comparison test. *p<0.05; **p<0.01; ***p<0.001; ****p<0.0001. C) Relationship between CD19, CD81, CD20 and CD69 in bone marrow B cells of hu-mice. Autoreactive and nonautoreactive immature B cells and pro-B/pre-B cells were gated within the bone marrow $CD24^{hi}CD38^{hi}$ cell population of HIS hu-mice as shown in top plots. Plots in middle row show a representative analysis of CD19 vs CD81 expression on κ^+AUT immature B cells from a Hcκ+ hu-mouse (left), and on κ^+NA immature B cells (center) and $IgM^-Ig\kappa^-$ pro-B/pre-B cells (right) from a Hcκ– hu-mouse gated as shown on top row. Plots in bottom row show expression of CD20 vs CD69 on $CD81^-$ and $CD81^+$ cell subsets gated as in middle row. These plots are representative of N=10 Hcκ+ and 13 Hcκ– hu-mice, respectively.

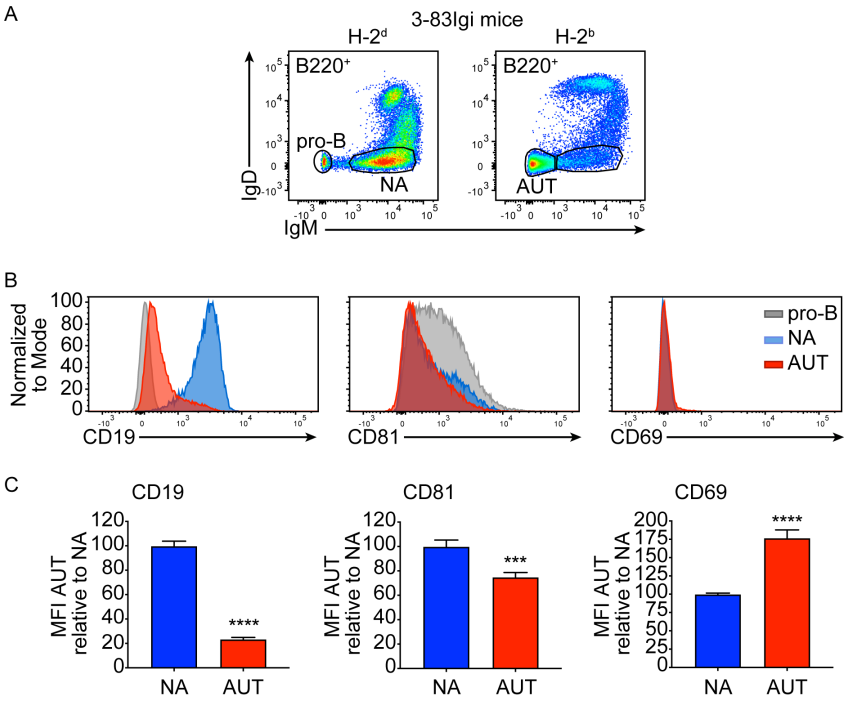

Fig. S2. Expression of CD19, CD69 and CD81 on autoreactive and nonautoreactive mouse immature B cells

Analysis of bone marrow immature B cells from 3-83Igi mice on the H-2^{d} nonautoreactive or the H-2^{b} autoreactive background. A) Representative pseudocolor plots showing B220^{+} gated B cells analyzed for IgM and IgD expression to discriminate IgM^{-}IgD^{-} pro-B cells and IgM^{+}IgD^{-} nonautoreactive immature B cells in 3-83Igi,H-2^{d} mice, and IgM^{-}IgD^{-} autoreactive immature B cells (including few pro-B cells) in 3-83Igi,H-2^{b} mice. B) Representative histogram plots of CD19, CD81, and CD69 staining on pro-B cells, and on nonautoreactive and autoreactive immature B cells. C) MFIs of CD19, CD81 and CD69 for autoreactive immature B cells are shown relative to those of nonautoreactive immature B cells analyzed on the same day. N=9 for each group of mice. Statistical analysis was performed by one-tailed *t* tests with Welch's correction. ***p<0.001; ****p<0.0001.

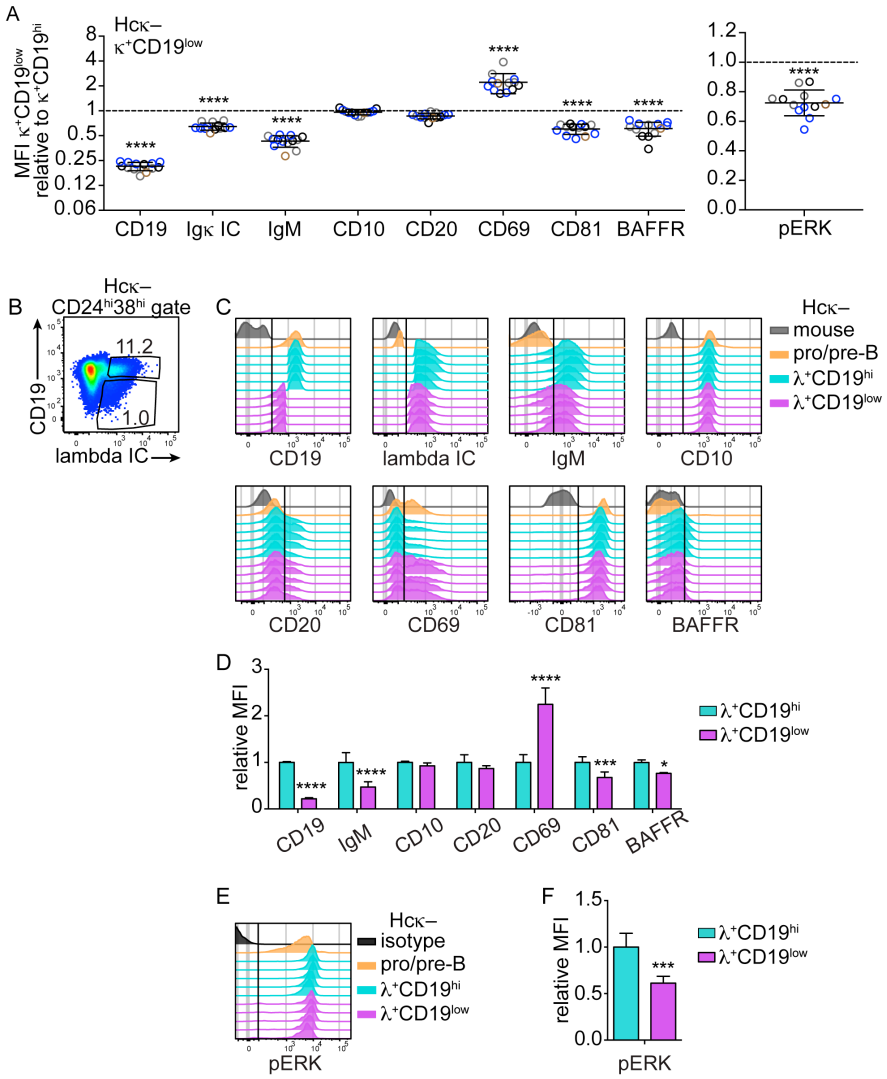

Fig. S3. Human CD19^{low} κ^{+} and λ^{+} immature B cells from Hcκ– hu-mice display a phenotype consistent with autoreactivity.

A) Relative MFIs of indicated molecules expressed by κ^{+}CD19^{low} immature (CD24^{hi}CD38^{hi}) B cells of individual Hcκ– hu-mice. The relative MFIs were calculated by dividing the MFI value of each sample by the average MFI of the κ^{+}CD19^{hi} samples from the Hcκ– hu-mice that were analyzed on the same day. N=13 Hcκ– mice from 4 groups generated with distinct cord blood units. B) Gating strategy for CD19^{low} and CD19^{hi} λ^{+} immature B cells within the human CD24^{hi}CD38^{hi} bone marrow cell population of Hcκ–

HIS hu-mice. The $CD24^{hi}CD38^{hi}$ cells were gated as shown in Figs. 1A and S1A. C) Histogram plots comparing the expression of indicated markers by $CD19^{low}$ and $CD19^{hi}$ λ^+ immature B cells from Hcκ– hu-mice. Each histogram represent an individual mouse from a group of littermates transplanted with the same cord blood unit. D) Relative MFI of indicated markers (as shown in panel "C") among the human $CD19^{low}$ and $CD19^{hi}$ λ^+ ($CD24^{hi}CD38^{hi}$) immature B cells from Hcκ– hu-mice generated with the same cord blood unit. E,F) Flow cytometric analyses of pERK levels in pervanadate-treated human B cell subsets from Hcκ– hu-mice (E), and statistical analysis of pERK MFI in λ^+ immature B cells (F). Each histogram in "E" represents a mouse and the isotype control shows $CD38^{hi}$ cells. The MFIs for graphs in panels "D" and "F" were normalized by dividing the MFI values of $CD19^{hi}$ or $CD19^{low}$ λ^+ cells of individual mice to the average MFI of $CD19^{hi}$ λ^+ cells from hu-mice analyzed on the same day. Results in all graphs are expressed as mean and SD. N=6 Hcκ– hu-mice from two groups of animals transplanted with distinct cord blood units. Statistical analysis was performed with two-way ANOVA multiple comparison test. *$p<0.05$; ***$p<0.001$; ****$p<0.0001$.

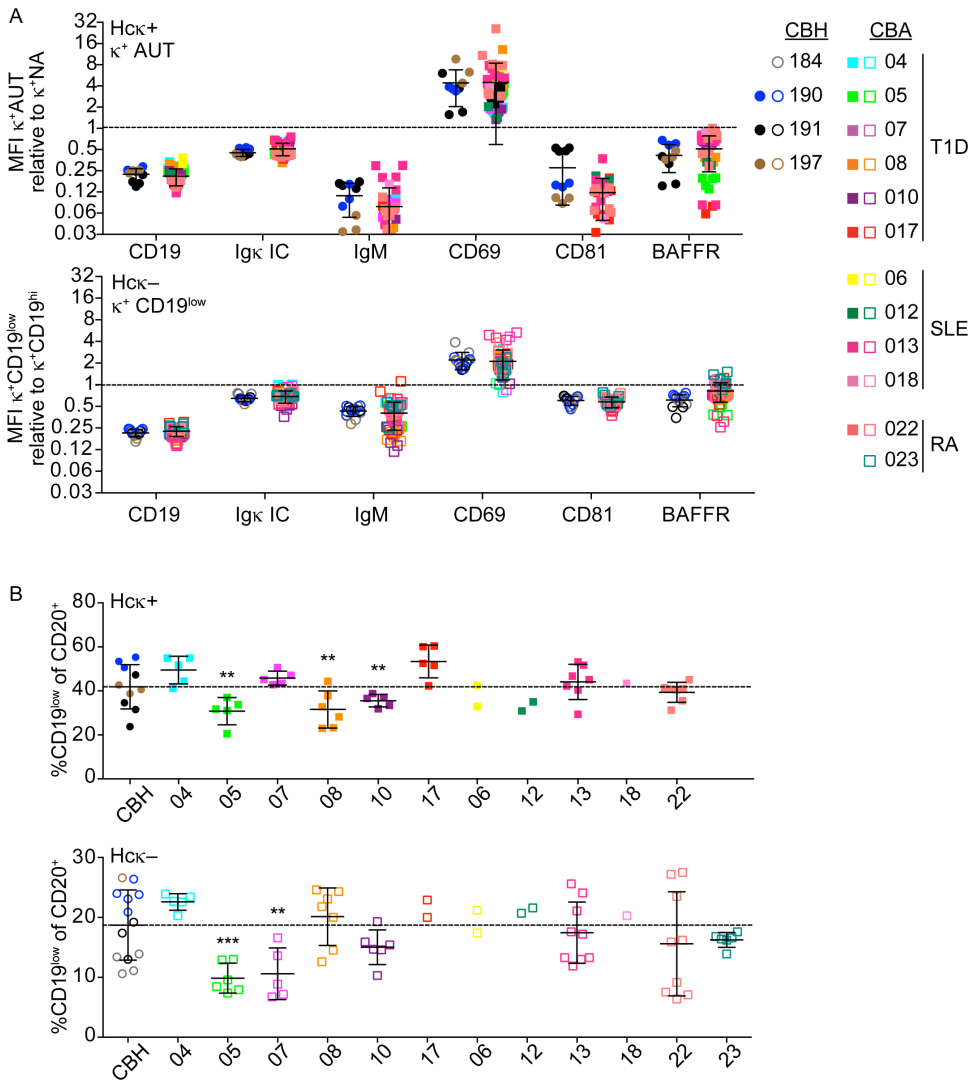

Fig. S4. Expression of tolerance markers on CD19^{low} κ^{+} human immature B cells from HIS hu-mice generated with cord bloods from infants of either healthy or autoimmune mothers.

HIS hu-mice were generated with HSCs enriched from cord blood samples collected from newborns of either healthy or autoimmune mothers. A) Relative MFI of indicated markers among the CD19^{low} κ^{+} human immature B cells from Hcκ+ hu-mice (top) or Hcκ– hu-mice (bottom) that were generated with cord blood from newborns of either "healthy" (CBH, circles) or "autoimmune" (CBA, squares) mothers. CD19^{low}

$CD24^{hi}CD38^{hi}$ immature B cells were gated as shown in Figs. 1A,B and 2A. B) Frequency of $CD19^{low}$ cells within the $CD20^{+}CD24^{hi}CD38^{hi}$ bone marrow B cell population of Hcκ+ (top) or Hcκ– (bottom) hu-mice that were generated with cord blood from newborns of either “healthy” (CBH, circles) or “autoimmune” (CBA, squares) mothers. Filled and empty symbols represent Hcκ+ and Hcκ– hu-mice, respectively. Different colors represent distinct cord blood donors and their related disease, as shown in legend and in Table S1. Results are expressed as mean±SD. N=10 Hcκ+ and 13 Hcκ– hu-mice generated with 3 or 4 different CBH samples, respectively. N=53 Hcκ+ hu-mice and 58 Hcκ– hu-mice generated with HSCs from 11 or 12 CBA individual cord blood samples, respectively. CD81 was not measured in hu-mice generated with CBA samples 04, 05, 07, 08, 010, and BAFFR was not measured in hu-mice generated with CBA-04. Statistical analysis was performed with two-way ANOVA multiple comparison test. **$p<0.005$.

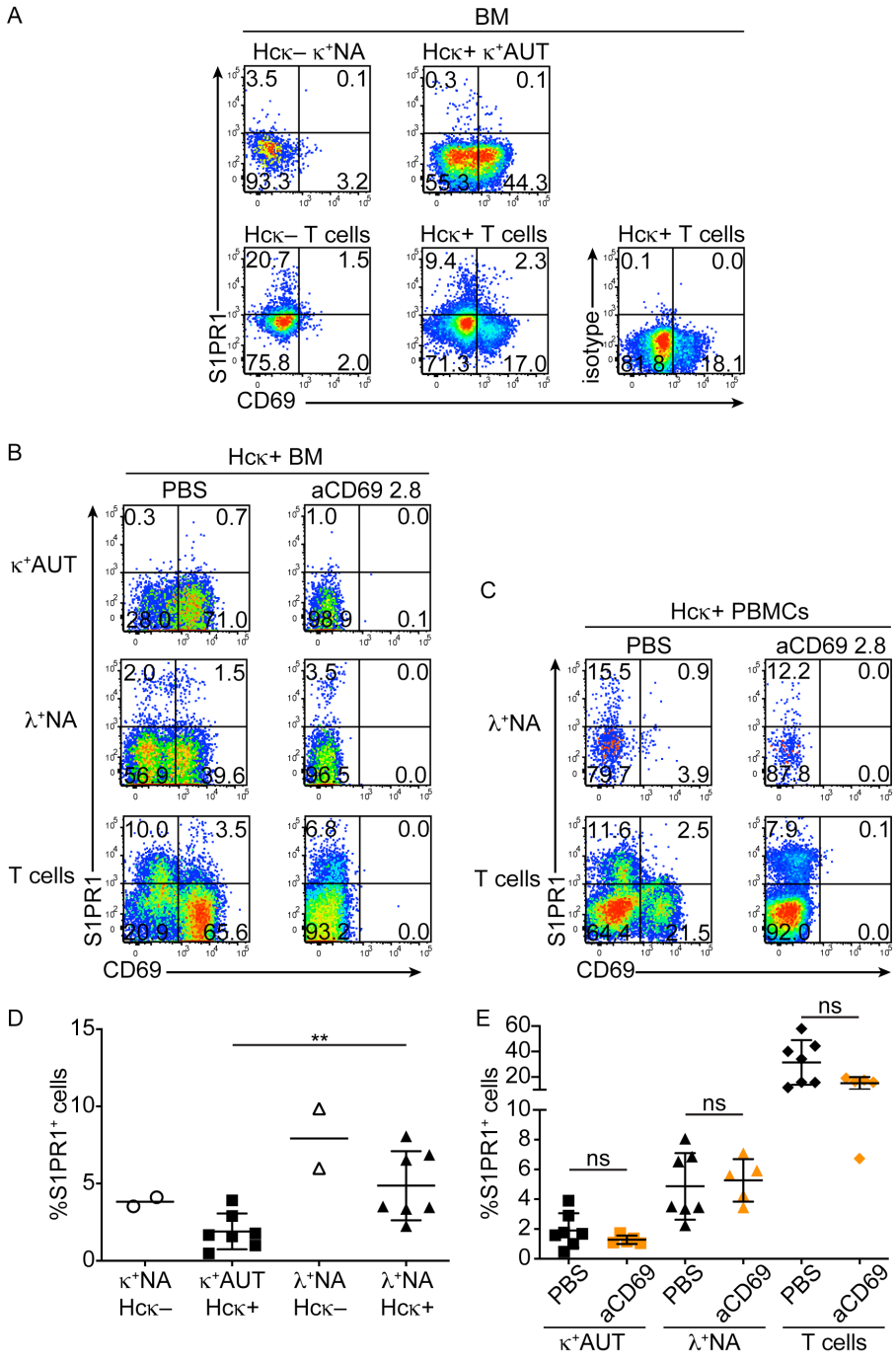

Fig. S5. Expression of S1PR1 on B cells and T cells from HIS hu-mice.

A-C) Bone marrow cells and PBMCs from Hcκ+ and Hcκ– hu-mice, either not treated (A) or injected with anti-hCD69 mAb 2.8 or PBS (B, C), were analyzed by flow cytometry for surface expression of S1PR1 (or isotype control) and CD69. Human T cells were gated as hCD45$^+$CD3$^+$, while nonautoreactive (NA) immature B cells were

hCD45^{+}CD38^{high}CD24^{high} and either κ^{+}CD19^{high} or IgM$^{+}\kappa^{-}$CD19^{high} for κ^{+} and λ^{+} cells, respectively. Autoreactive (AUT) immature B cells were hCD45^{+}CD38^{high}CD24^{high} and κ^{+}CD19^{low}. Igλ^{+} cells from PBMCs (C) were also gated as CD20^{+}. D,E) Graphs show the frequency of S1PR1^{+} cells within the indicated cell populations from either Hcκ+ and Hcκ– hu-mice untreated or treated with PBS (D and E), or treated with anti-hCD69 mAb 2.8 (E). N=7 Hcκ+ hu-mice, 6 of which treated with PBS. N=5 Hcκ+ hu-mice treated with anti-hCD69. N=2 Hcκ– hu-mice, one of which treated with PBS. Mice were analyzed over 5 independent experiments. Statistical analysis was performed with unpaired two-tailed *t* test with Welch's correction. **p<0.01, ns=not significant.

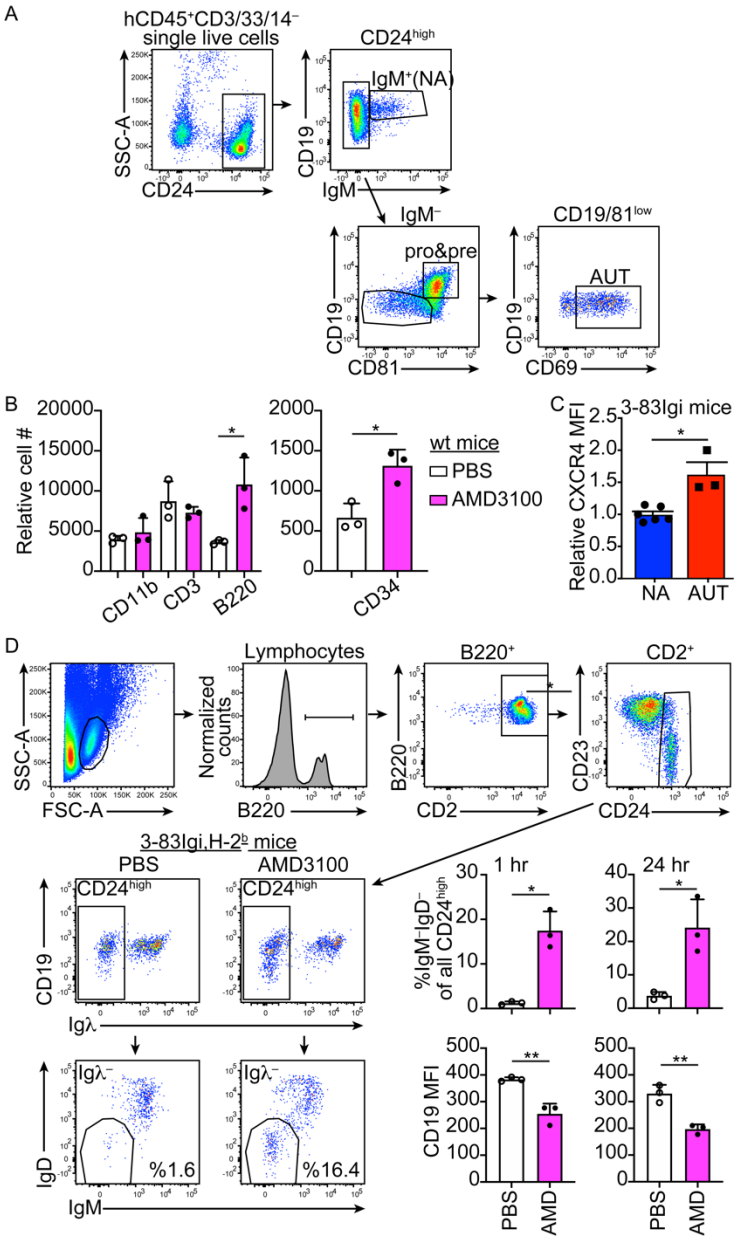

Fig. S6. Gating strategy for hu-mouse cells migrating to CXCL12, and CXCR4 blockade in autoreactive 3-83Igi,H-2^{b} mice.

A) Flow cytometric gating strategy for the analysis of B cells migrating to CXCL12 shown in main Fig. 6C. Bone marrow cells from Hcκ+ hu-mice were recovered from upper and lower wells of transwell plates and analyzed as shown to gate CD19^{high}IgM^{+} nonautoreactive (NA) immature B cells, CD19^{high}IgM^{-}CD81^{high} pro&pre-B cells, and

$CD19^{low}IgM^{-}CD81^{low}CD69^{+}$ autoreactive (AUT) immature B cells. AUT and NA cells were discriminated based only on differences of cell surface markers to reduce cell manipulation and loss during cell staining. B) Functional test of AMD3100 treatment. CB17,H-2^{b} wild-type mice (3 per group) were injected with PBS or AMD3100 and euthanized after one hour for analyses. Cells were isolated from the same volume of blood from each mouse, stained for B220, CD3, CD11b, and CD34 and collected on the flow cytometer. The graphs report number of cell events collected over 60 sec for each of the marker-positive populations. C) Analysis of CXCR4 expression on $B220^{+}IgD^{-}$ bone immature B cells from 3-83Igi,H-2^{d} nonautoreactive (NA) and 3-83Igi,H-2^{b} autoreactive (AUT) mice. D) Analysis of autoreactive B cells in blood of treated mice. 3-83Igi,H-2^{b} mice (3 per group) were injected with PBS or AMD3100 either once and euthanized after one hour, or 4 times over the course of 24 hours and euthanized one hour after the last injection. Blood cells were stained and analyzed to serially gate on cells that were $B220^{+}CD2^{+}CD24^{high}Ig\lambda^{-}$ and $IgM^{-/low}IgD^{-}$, which represent autoreactive immature B cells in these animals. Numbers in the bottom IgDvsIgM flow plots are frequencies of $IgM^{-/low}IgD^{-}$ gated cells within total $CD24^{high}$ cells. The graphs show the frequency of autoreactive immature B cells among all $CD24^{high}$ B cells (top), and the CD19 MFI of $CD24^{high}Ig\lambda^{-}$ cells (bottom) in mice treated for one hour (left) or 24 hours (right). Statistical analyses were performed with a two-tailed Student's *t* test. *$p<0.05$; **$p<0.01$.

Table S1. Demographic of pediatric bone marrow biopsy specimens

ID#	Sex	Age (years)
BM-04	M	15
BM-05	M	6
BM-07	F	8
BM-08	M	4
BM-12	M	15
BM-13	M	2
BM-15	M	0.7
BM-16	M	14
BM-17	M	7
BM-18	M	16
BM-20	M	4
BM-21	F	4

Table S2. Demographic and genetic details of autoimmune cord blood donors

ID#	Mother's Autoimmunity (yrs from diagnosis)	Mother's Race/Ethnicity	Infant Gender	Autoimmunity in other family members	PTPN22 allele
CBA-04	T1D (27)	White/N/A	M	Y	R620
CBA-05	T1D (18)	White/Not hispanic	F	Y	**W620**
CBA-06	SLE (5)	More than one/Not Hispanic	M	N	R620
CBA-07	T1D (19)	Asian/Not hispanic	M	N/A	R620
CBA-08	T1D (20)	White/Hispanic	M	Y	R620
CBA-010	T1D (16)	White/Not hispanic	M	Y	R620
CBA-012	SLE (6)	Black/Not hispanic	M	Y	R620
CBA-013	SLE (10)	White/Hispanic	F	Y	R620
CBA-017	T1D (7)	White/Hispanic	F	N/A	R620
CBA-018	SLE (3)	White/Not hispanic	F	Y	R620
CBA-022	RA (16)	White/Not hispanic	F	Y	R620
CBA-023	RA (4)	White/Not hispanic	M	N	R620

SI References

1. E. Eliopoulos *et al.*, Association of the PTPN22 R620W polymorphism with increased risk for SLE in the genetically homogeneous population of Crete. *Lupus* **20**, 501-506 (2011).
2. J. Lang, N. Weiss, B. M. Freed, R. M. Torres, R. Pelanda, Generation of hematopoietic humanized mice in the newborn BALB/c-Rag2null Il2rgammanull mouse model: a multivariable optimization approach. *Clin Immunol* **140**, 102-116 (2011).
3. J. Lang *et al.*, Studies of lymphocyte reconstitution in a humanized mouse model reveal a requirement of T cells for human B cell maturation. *J Immunol* **190**, 2090-2101 (2013).
4. N. Legrand *et al.*, Functional CD47/signal regulatory protein alpha (SIRP(alpha)) interaction is required for optimal human T- and natural killer- (NK) cell homeostasis in vivo. *Proc Natl Acad Sci U S A* **108**, 13224-13229 (2011).
5. J. Lang *et al.*, Replacing mouse BAFF with human BAFF does not improve B-cell maturation in hematopoietic humanized mice. *Blood Adv* **1**, 2729-2741 (2017).
6. J. Lang *et al.*, Receptor editing and genetic variability in human autoreactive B cells. *J Exp Med* **213**, 93-108 (2016).
7. E. Esplugues *et al.*, Induction of tumor NK-cell immunity by anti-CD69 antibody therapy. *Blood* **105**, 4399-4406 (2005).
8. A. O. Cuff *et al.*, Eomeshi NK Cells in Human Liver Are Long-Lived and Do Not Recirculate but Can Be Replenished from the Circulation. *J Immunol* **197**, 4283-4291 (2016).
9. N. Capitani *et al.*, S1P1 expression is controlled by the pro-oxidant activity of p66Shc and is impaired in B-CLL patients with unfavorable prognosis. *Blood* **120**, 4391-4399 (2012).
10. E. E. Donovan, R. Pelanda, R. M. Torres, S1P3 confers differential S1P-induced migration by autoreactive and non-autoreactive immature B cells and is required for normal B-cell development. *Eur J Immunol* **40**, 688-698 (2010).
11. T. C. Beck, A. C. Gomes, J. G. Cyster, J. P. Pereira, CXCR4 and a cell-extrinsic mechanism control immature B lymphocyte egress from bone marrow. *J Exp Med* **211**, 2567-2581 (2014).
12. M. Mandal *et al.*, CXCR4 signaling directs Igk recombination and the molecular mechanisms of late B lymphopoiesis. *Nat Immunol* **20**, 1393-1403 (2019).
13. R. Pelanda *et al.*, Receptor editing in a transgenic mouse model: site, efficiency, and role in B cell tolerance and antibody diversification. *Immunity* **7**, 765-775 (1997).
14. R. Halverson, R. M. Torres, R. Pelanda, Receptor editing is the main mechanism of B cell tolerance toward membrane antigens. *Nat Immunol* **5**, 645-650 (2004).